

Study of diopside ceramics for biomaterials

TORU NONAMI*

National Industrial Research Institute of Nagoya, 1-1 Hirate-cho, Kita-ku, Nagoya-shi, 462 Japan

SADAMI TSUTSUMI

Kyoto University, Kawahara-cho, Shogoin, Sakyo-ku, Kyoto-shi, 606 Japan

Diopside was prepared by sintering a powder compact of composition $\text{CaO} - \text{MgO} - 2\text{SiO}_2$ at 1300°C for 2 h. The bending strength of diopside was 300 MPa and the fracture toughness was $3.5 \text{ MPa m}^{1/2}$. It was proved that diopside has no general toxicity in cell culture.

Diopside implanted in rabbits came in close contact with the newly grown bone. X-ray microanalysis spectral diagrams show a change of composition across the junction from the diopside to the newly grown bone. High-resolution transmission electron microscopy revealed crystal growth at the interface between diopside and the newly grown bone, and continuity between diopside lattices and those of the new crystals.

© 1999 Kluwer Academic Publishers

1. Introduction

Ceramics have been used as materials for artificial bone [1–7]. Having biological affinity, calcium phosphate based ceramics, primarily hydroxyapatite (HAp) and tricalcium phosphate are used as biomaterials. However, due to their poor mechanical properties, in particular their low fracture toughness, they cannot be used under a heavy load and their application is limited [8–20].

To increase the fracture toughness of sintered HAp, the composite of diopside ($\text{CaO} - \text{MgO} - 2\text{SiO}_2$) and HAp was fabricated [21]. The bending strength and fracture toughness of the sintered diopside–HAp composite were two or three times higher than those of sintered HAp, and it was proved that the composite had no general toxicity in cell culture test [22]. In this study, to clarify the physical properties and biocompatibility of diopside ceramics [23], mechanical properties, *in vitro* and *in vivo*, etc., were examined and we discovered that sintered diopside has high mechanical strength and shows satisfactory biological activity.

2. Materials and methods

2.1. Material preparation

The material diopside was prepared by weighing out the specified quantities of CaCO_3 , MgO and SiO_2 of a guaranteed grade (Junsei Kagaku Co.), mixing them, calcining them at 1100°C for 2 h and wet grinding them for 90 min in a medium stirring mill (Sand Mill, Kansai Paint Co.) using zirconia balls 2 mm in diameter.

To obtain sintered diopside (hereafter named diopside), the cake was dried and molded under 5 MPa and fired in air at 1300°C for 2 h.

HAp powder was synthesized by precipitation [24].

The sintered HAp was prepared by hot-isostatic pressing at 203 MPa and 1100°C for 2 h.

The diopside and HAp were identified by powder X-ray diffraction (XRD; XD-D1, Shimazu Seisakujo Co.).

2.2. Evaluation of properties

To measure flexural strength, bending test samples ($2 \times 3 \times 20 \text{ mm}^3$) chamfered and mirror polished with diamond paste were used. Bending strength was applied normally with a strength testing machine (Servo-Pulser EHF-F1, Shimazu Seisakujo Co.) under the condition of a crosshead speed of 0.5 mm min^{-1} and a span of 15 mm. Ten samples were tested and a mean was obtained. The fracture toughness was evaluated by the single-edge-precracked-beam (SEPB) method [25], abiding by Japanese industrial standards [26]. To measure fracture toughness, the bending test samples were notched 0.5 mm deep with a 0.1-mm-thick diamond wheel, and tested for three-point bending with a strength testing machine with a crosshead speed of 0.5 mm min^{-1} . The same tests were conducted ten times with ten samples, and a mean was obtained and determined as for the fracture toughness of the samples. Young's modulus and Poisson's ratio were measured on samples of $80 \times 2 \times 20 \text{ mm}^3$ using the ultrasonic pulse echo method. The apparent density of diopside was measured in water using the Archimedeian technique. The sintered samples were pulverized into powder having a surface area of $5 \text{ m}^2 \text{ g}^{-1}$, which was used to determine the true density. The relative density was calculated from the apparent and true densities.

A sample having a surface area of 200 mm^2 was placed in 200 ml of an aqueous solution of lactic acid at pH 4 for 48 h at 36.5°C (in a constant temperature bath) and was

*Author to whom correspondence should be addressed.

slightly shaken. The samples were taken out, rinsed and dried to measure weight loss. The same test was performed with a physiological salt solution.

2.3. Evaluation of affinity with cells

Diopside, HAp, pure titanium and polystyrene as control (P-DISH) were used for the experiment. These materials were molded into discs, 30 mm in diameter and 1 mm thick, and their surfaces were polished to a surface roughness of 1 μm or less.

L-929 (ATC, CCL1 NCTC clone 929 strain) was used for the culture cells. A 10% FCS added Eagle MEM culture medium was used to culture osteoblast and fibroblast, respectively. To obtain the initial cell adhesion ratio, 1×10^5 culture cells after three days of generation growth were sown on a disc and were cultured for 5 h. The cells were then counted. The cell propagation rates were obtained by soaring 2×10^5 of the same cells on a disc and collecting cells after one, two and three days.

2.4. Biological properties

Rectangular diopside specimens ($3 \times 4 \times 6 \text{ mm}^3$) were implanted into holes ($3 \times 4 \times 6 \text{ mm}^3$) formed in the lower edge of the jaw bone of adult male rabbits, weighing from 2.2. to 2.8 kg and left for 12 weeks.

A diopside dental root implant (10 \times 4 mm in diameter) was implanted into a cavity in the mandible of a Japanese monkey and left for six months. To prepare the bone cavity, we extracted the mandibular first molar and left it for three months. After the socket bone was repaired, a cavity (10 mm deep, 4 mm in diameter) was bored by means of dental bars.

After the respective waiting periods, the animals were anaesthetized, and perfusion fixation was performed. Specimens were taken out, dehydrated with ethanol and embedded in polyester resin (Rigolac, Oken Shoji Co., Tokyo). These samples were then embedded in epoxy resin and cut into sections. Scanning electron microscope (SEM; H-600, Hitachi, Tokyo) and high-resolution transmission electron microscope (EM-002B, Topcon Co.) analyses and X-ray microanalyses (XMA) were taken of the interface between the implant and the newly grown bone to study the biocompatibility of the implant. The same interface was analyzed with a microbeam X-ray diffractometer (50 kV at 40 mA). The X-ray irradiation area was 250 nm in diameter. In addition, qualitative and quantitative analyses (weight per cent) of Ca and P in the same area were performed by means of an electron-dispersive X-ray microanalyzer attached to an electron microscope (Kevex 7000, Kevex, USA; H-600, Hitachi), and the Ca/P atomic ratio was calculated. The area analyzed was about 30 nm in diameter.

3. Results and discussion

3.1. The diopside material

The XRD pattern of diopside is shown in Fig. 1. Only diopside peaks were detected by XRD.

Bending strength, fracture toughness, Young's modulus, Poisson's ratio, relative density and acid resistance of diopside and HAp are shown in Table I. It is found that

diopside is more unlikely to fracture and more durable than HAp. The weight loss of diopside in an aqueous solution of lactic acid and physiological salt solution was less than that of HAp.

3.2. Cell culture tests

Diopside was submitted to cell culture tests. There were no significant differences in the initial cell adhesion ratios between diopside, titanium, HAp and P-DISH. Fig. 2 illustrates the growth curves of cells cultured on

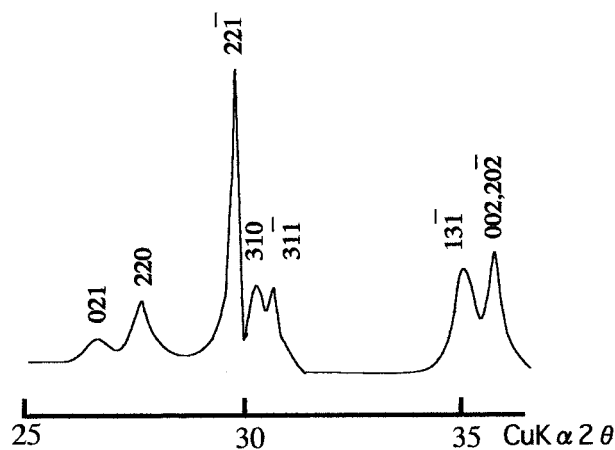


Figure 1 X-ray diffraction of diopside sintered at 1300°C for 2 h.

TABLE I Properties of diopside and HAp

	Diopside	HAp
Composition, %		
CaO	25.9	55.8
MgO	18.0	0
SiO ₂	55.5	0
P ₂ O ₅	0	42.4
Bending strength, MPa	300	110
Fracture toughness, MPa m ^{1/2}	3.5	1.1
Young's modulus, GPa	170	47
Poisson's ratio	0.35	0.27
Weight loss, %		
Soaked in lactic acid	2.8	16.5
Soaked in physiological salt solution	0.05	0.13
Density, g cm ⁻³	3.20	3.16

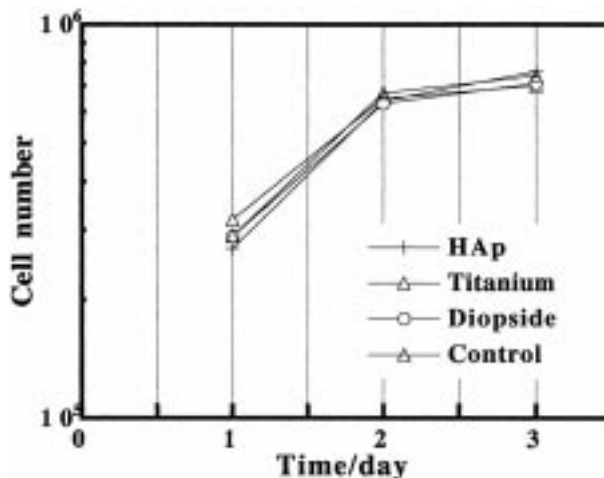


Figure 2 Growth curves of cells cultured on control (P-Dish), titanium, diopside and HAp.

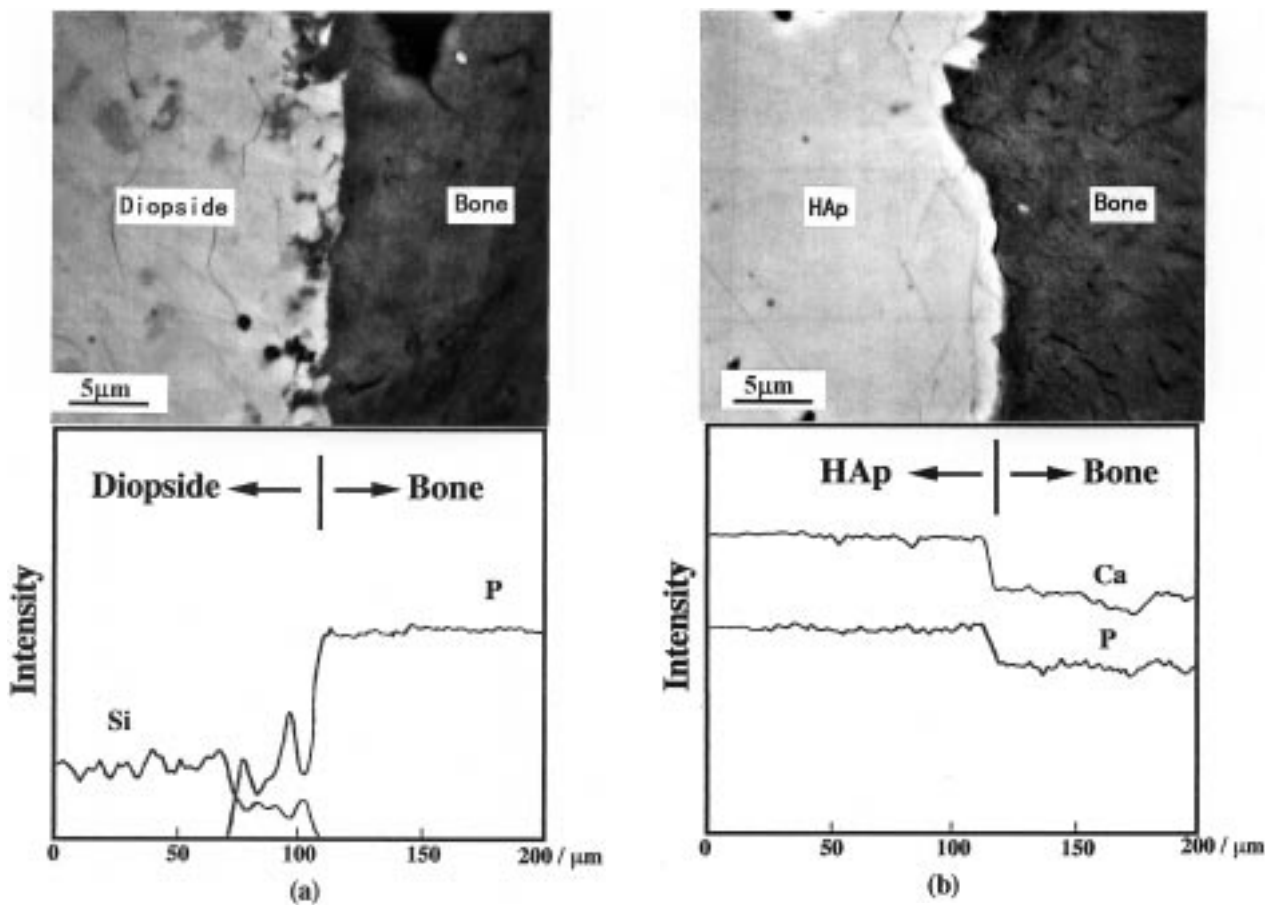


Figure 3 SEM photographs and XMA patterns of the interface 12 weeks after implantation: (a) diopside, and (b) HAp.

diopside, HAp, titanium and P-DISH. All samples exhibited similar changes. The results of the cell culture tests above showed that diopside is harmless.

3.3. Biological properties

3.3.1. Diopside rectangular implant in a rabbit bone cavity

Twelve weeks after implantation diopside came in contact with newly grown bone. Fig. 3 shows SEM photographs and XMA patterns of the interface between diopside and bone (a), and HAp and bone (b). An XMA spectral diagram shows the change of composition across the junction of the diopside with the newly grown bone after 12 weeks. It can be seen that the components of an intermediate layer between the newly grown bone and the diopside have a gradient of concentration. Fig. 4 presents microbeam XRD patterns of a portion on the interface and inside the diopside. Both diopside and apatite phases are formed on the interface.

3.3.2. Diopside dental root implant in a monkey bone cavity

At the interface between diopside and newly grown bone, many needle- or platelet-shaped crystals were observed by SEM as shown in Fig. 5. In cross-section, these crystals showed a platelet shape about 2.5 nm thick and about 20 nm wide (Fig. 5b) or a hexagonal prism about 7 nm thick and about 1.5 nm wide (Fig. 5c); the maximum lattice spacing was about 0.82 nm for both

arrangements. Lattice spacing sets at about 0.82-nm intervals, crossed each other at 120° (Fig. 5b and c). The crystals came in contact with diopside, and crystal lattices running in the same direction were partially continuous with each other (Fig. 5a, d). Selected area electron diffraction of new crystals showed the diffraction pattern of apatite (Fig. 5d).

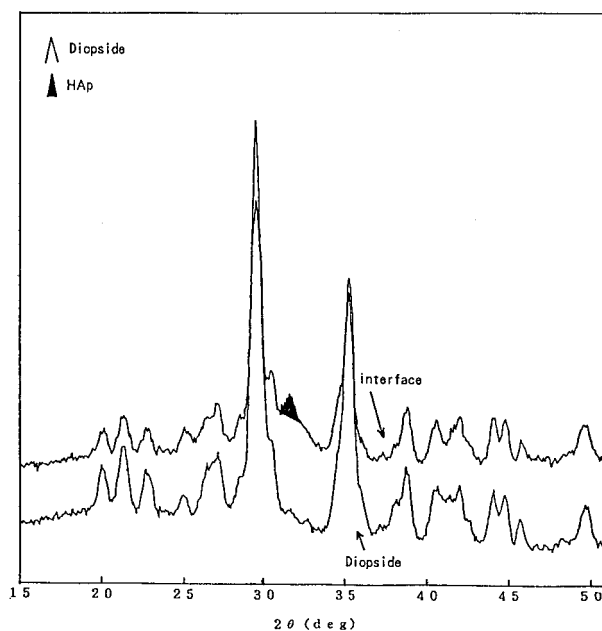


Figure 4 Microbeam XRD patterns of a portion on the interface and inside the diopside 12 weeks after implantation.

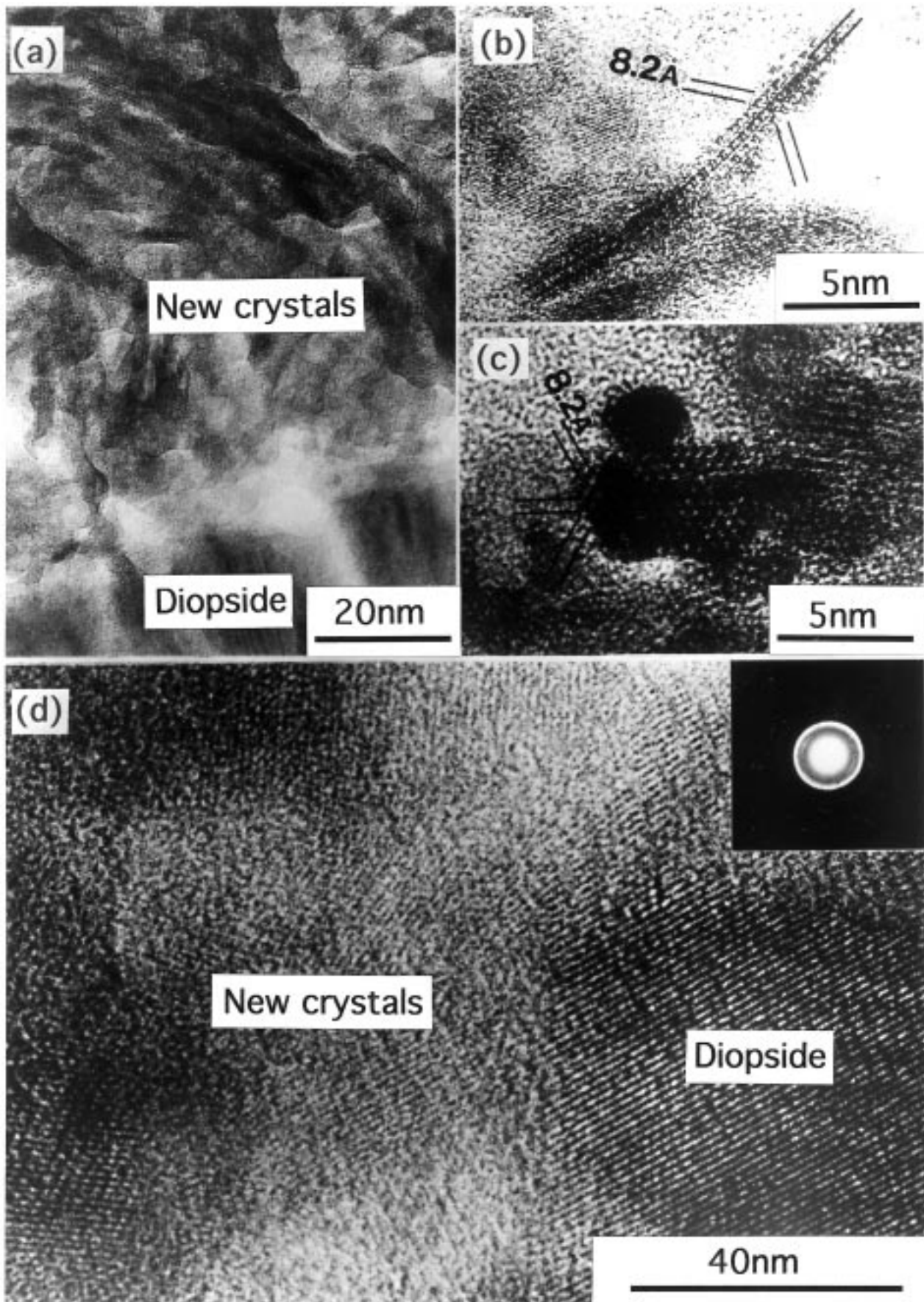


Figure 5 High-resolution transmission electron micrographs of diopside implanted into the monkey bone cavity and left for six months: (a) interface between diopside and new crystals; (b, c) cross-sections of new crystals, (d) interface between diopside and new crystals, and selected area electron diffraction of the new crystal.

The new crystals morphologically resembled those in bone and dentin [27], and the lattice spacing of 0.82 nm, which crossed each other at 120°, corresponds to the *c*-axis plane of apatite. The results of selected area electron diffraction also suggested apatite formation.

Qualitative analysis showed peaks of P and Ca in the new crystals around the diopside. Quantitative analysis of the new crystals revealed a Ca/P atomic ratio of 1.65 ± 0.06. The Ca/P atomic ratio of the new crystals was close to the theoretical value for apatite (1.67).

A few thick crystals were also observed. Such crystals have also been observed in dentin and are considered to be a general morphological type of crystal. Their morphology suggests that these crystals formed as a result of growth in the direction of the *a*-axis.

The apatite that was formed in the diopside surface layer is similar to the apatite in bone. Apatite in bone shows low crystallinity and has a large surface area due to small crystals, and is thus highly reactive [28]. Therefore, this result may suggest that highly reactive apatite crystallizes at the diopside surface and forms an apatite layer by reacting with body fluid, thus promoting binding with the surrounding bone [29].

4. Conclusions

In this study we examined the physical properties and biocompatibility of diopside. Diopside was prepared by sintering a powder compact of composition CaO – MgO – 2SiO₂ at 1300 °C for 2 h. The bending strength of diopside was 300 MPa and the fracture toughness was 3.5 MPa m^{1/2}. These values were about two or three times higher than those of HAp. The weight loss of diopside in an aqueous solution of lactic acid and physiological salt solution were less than those of HAp. In the experiment, which used rabbits and monkeys, diopside forms a uniform junction with newly grown bone. High-resolution transmission electron microscopy revealed crystal growth at the interface between diopside and the newly grown bone, and continuity between the diopside lattice and that of the new crystals. The morphological characteristics of the new crystals and the results of microbeam XRD, selected area electron diffraction and EDX suggest that these new crystals are apatite. It is expected that diopside is useful for artificial bones and dental roots etc.

Acknowledgments

The authors would like to thank Professor H. Noma, Dr Yajima and Dr Y. Miake of Tokyo Dental College for their animal euthanasia and implantation control. This study was supported in part by Dr H. Ohsato of Nagoya Institute of Technology and TDK Co., Ltd.

References

1. L. F. PELTIER, *Clin. Orthop. Rel. Res.* **21** (1961) 1.
2. L. SMITH, *Arch. Surg.* **87** (1963) 653.
3. P. BOUTIN, *Rev. Chir. Orthop.* **58** (1972) 229.
4. S. F. HULBERT, L. L. HENCH, D. FORBERS and L. S. BOWMAN, *Ceram. Int.* **8** (1992) 131.
5. S. FUJIMURA, M. YOSHIMURA, T. HATTORI, H. AOKI, M. UCHIDA and S. SOMIYA, *J. Ceram. Soc. Jpn* **95** (1987) 753.
6. K. ITOH, M. YOSHIMURA and S. SOMIYA, *ibid.* **96** (1988) 109.
7. Y. HIRAYAMA, H. IKATA, H. AKIYAMA, K. NAGANUMA, S. OJIMA and M. KAWASAKI, in "Proceeding of the International Institute for the Science of Sintering (IISS) Symposium", edited by S. Somiya, M. Shimada, M. Yoshimura and R. Watanabe (Elsevier, 1988) p. 1332.
8. S. N. BHASHAR, D. E. CUTRIGHT, M. J. KNAPP, J. D. BEASLEY, P. BIENVENIDE and T. D. BRISHELL, *ORAL SURG.* **31** (1971) 282.
9. J. R. STRUB and T. W. GABERTHUEL, *Schweizmschr. Zahnheik* **88** (1978) 798.
10. J. JARCHO, J. F. KAY, K. I. GUMAER, R. H. DOREMUS and H. P. DROBECK, *J. Bioengng* **1** (1977) 79.
11. E. B. NERY and K. L. LYNCH, *J. Periodontol.* **49** (1978) 523.
12. L. L. HENCH, R. J. SPLINTER, W. C. ALLEN and T. K. GREENLEE, JR, *J. Biomed. Mater. Res.* **6** (1972) 117.
13. H. W. DENISSEN, K. DE GROOT, P. C. MAKKES, A. VAN DEN HOOF and P. J. KLOPPER, *ibid.* **14** (1980) 713.
14. H. W. DENISSEN, A. A. H. VELDHUIS, P. C. MAKKES, A. VAN DEN HOOF and K. DE GROOT, *Clin. Prevent. Dent.* **2** (1980) 23.
15. K. DE GROOT, *J. Biomaterials* **1** (1980) 47.
16. M. JARCHO, C. H. BOLEN, M. B. THUMAS, J. BOBICK, J. F. KAY and R. H. DOREMUS, *J. Mater. Sci.* **11** (1976) 2027.
17. M. AKAO, N. MIURA and H. AOKI, *J. Ceram. Soc. Jpn* **92** (1984) 78.
18. M. TORIYAMA, S. KAWAMURA and S. SHIBATA, *ibid.* **95** (1987) 92.
19. M. MONMA, T. KAMIYA, M. TSUTSUMI and Y. T. HASEGAWA, *Gypsum Lime* **208** (1987) 127.
20. N. TAMARI, I. KONDO and M. KINOSHITA, "Sintering of Hydroxyapatite by Hot-pressing and Their Mechanical Properties", Government Industrial Research Osaka Kiho, No. 38 (1987) 71.
21. T. NONAMI, *MRS Symp. Proc.* **175** (1989) 71.
22. T. NONAMI and N. SATOH, *J. Ceram. Soc. Jpn* **103** (1995) 804.
23. T. NONAMI, *MRS Symp. Proc.* **252** (1992) 87.
24. T. KIJIMA and M. TSUTSUMI, *J. Amer. Ceram. Soc.* **62** (1979) 454.
25. J. E. SRAWLEY, *Int. J. Fract.* **12** (1976) 475.
26. Testing Method for Fracture Toughness of High Performance Ceramics, JIS R-1607, (Japanese Standards Association, 1990).
27. T. TAKUMA, H. TOHDA, K. WATANABE and S. YAMA, *J. Electron. Microsc.* **35** (1986) 60.
28. Y. KUBOKI and R. FUJISAWA, in "Bioscience and Biotechnology of Extracellular Matrix", edited by D. Fujimoto (IPC Press, Tokyo) pp. 220–38.
29. Y. MIAKE, T. YANAGISAWA, Y. YAJIMA, H. NOMA, N. YASUI and T. NONAMI, *J. Dent. Res.* **74** (1995) 1756.

Received 25 November 1997

and accepted 31 August 1998